HHS Public Access

Author manuscript

Nano Lett. Author manuscript; available in PMC 2020 February 17.

Published in final edited form as:

Nano Lett. 2019 March 13; 19(3): 1883–1891. doi:10.1021/acs.nanolett.8b04970.

Antibody-Armed Platelets for the Regenerative Targeting of Endogenous Stem Cells

Deliang Shen[†,‡,§,⊥], **Zhenhua Li**[*,‡,§,∥,⊥], **Shiqi Hu**[‡,§,⊥], **Ke Huang**[‡,§], **Teng Su**[‡,§], **Hongxia Liang**[†,‡,§], **Feiran Liu**[‡,§], **Ke Cheng**[*,†,‡,§]

[†]Department of Cardiology, The First Affiliated Hospital of Zhengzhou University, Zhengzhou, Henan 450052, China

[‡]Department of Molecular Biomedical Sciences and Comparative Medicine Institute, North Carolina State University, Raleigh, North Carolina 27607, United States

[§]Joint Department of Biomedical Engineering, University of North Carolina at Chapel Hill and North Carolina State University, Raleigh, North Carolina 27695, United States

[∥]College of Chemistry & Environmental Science, Hebei University, Baoding 071002, China

Abstract

Stem cell therapies have shown promise in treating acute and chronic ischemic heart disease. However, current therapies are limited by the low retention and poor integration of injected cells in the injured tissue. Taking advantage of the natural infarct-homing ability of platelets, we engineered CD34 antibody-linked platelets (P-CD34) to capture circulating CD34-positive endogenous stem cells and direct them to the injured heart. *In vitro*, P-CD34 could bind to damaged aortas and capture endogenous stem cells in whole blood. In a mouse model of acute myocardial infarction, P-CD34 accumulated in the injured heart after intravenous administration, leading to a concentration of endogenous CD34 stem cells in the injured heart for effective heart repair. This represents a new technology for endogenous stem cell therapy.

Graphical Abstract

[*]**Corresponding Authors**: zhenhuali@hbu.edu.cn; phone: +86-13331210907.; kcheng3@ncsu.edu; phone: +1-919-513-6157.

[⊥]Author Contributions

D.S., Z.L., and S.H. contributed equally.

Supporting Information

The Supporting Information is available free of charge on the ACS Publications website at DOI: 10.1021/acs.nanolett.8b04970. Additional details on synthesis and characterization and experimental procedures; figures showing SDS-PAGE analysis, the attachment of CD34 antibodies, surface marker expression, platelets and EPC binding, aggregometry assays, NRCM cell proliferation, representative TTC staining images, cytokine array analysis, numbers of platelets, flow cytometry analysis, Z-stack analysis, immune responses to P-CD34 injections, and F4/80-positive macrophages (PDF)

The authors declare no competing financial interest.

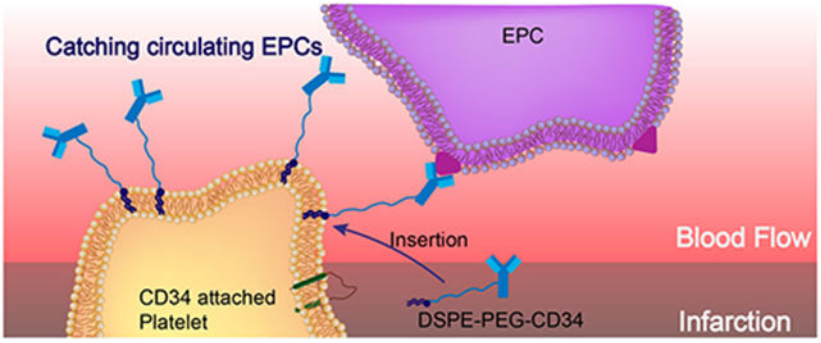

Keywords

Myocardium infarction; platelets; endogenous stem cells; antibodies

Cardiovascular disease (CVD) is a leading cause of death throughout the world.[1] Although therapeutic outcomes have been improved, new treatments are urgently needed to regenerate and repair the damaged heart due to the organ's lack of effective endogenous repair mechanisms.[2–4] Stem-cell-based therapies have rapidly emerged as promising treatment options for CVD. However, a major limitation is the low retention and integration of injected cells in the injured myocardium.[5–7] In addition, injected cells can be trapped in the lungs immediately after intravenous delivery.[8,9] Acute (within 24 h) cell retention in the heart is generally less than 10% regardless of the cell type and administration route. This may explain, at least in part, the marginal therapeutic benefit reported from cardiac cell therapy trials.[10,11] Despite the fact that local delivery of therapeutic cells is possible, minimally invasive delivery routes such as intravenous injection are more desirable.[12–14] Interestingly, endogenous stem cells are stimulated from the bone marrow and recruited to the heart after injury, but this natural repair process is insufficient to offset the progressive death of cardiomyocytes after a major myocardial infarction (MI), even with the presence of bone-marrow-stimulating agents such as granulocyte-colony-stimulating factor (G-CSF).[15] These findings have led us to speculate that despite endogenous stem cells are released from the bone marrow into the circulation, most are unable to home in on the injured myocardium to exert therapeutic benefits.[16] Thus, it is highly desirable to develop novel approaches to home endogenous stem cells to the injured heart.

Recently, owing to their important role as circulating sentinels for vascular damage, both platelets and their membrane derivatives have been widely used in the design of many functional nanocarriers for treating cancer and bacterial infection.[17,18] It has been well-established that acute MI can induce vascular damage and expose some subendothelial matrix, resulting in platelet recruitment. Previously, we reported that platelets and their membranes can be used for guiding infused stem cells to the injured heart.[19–22] Furthermore, previous studies confirmed that in acute coronary syndromes, platelets can bind to circulating $CD34^+$ progenitors in patients and enhance the adhesion of platelet-bound $CD34^+$ cells to the ischemic microcirculatory area to improve prognosis.[23] In the present work, we sought to apply a "take the cells out of cell therapy" strategy by fully relying on the manipulation of endogenous stem cells. To do that, we developed P-CD34 to

capture circulating CD34-positive cells and transport them to the heart injury site (Scheme 1). Due to their excellent biocompatibility, DSPE-PEG polymers were used as a linker between platelets and CD34 antibodies. Our findings suggest that infusion of those engineered regenerative platelets was able to exert a therapeutic benefit in a mouse model of acute MI.

P-CD34 Fabrication and Characterization.

To introduce CD34 antibodies to the surface of platelets, NHS-terminated DSPE-PEG was first covalently bonded to CD34 antibodies. DSPE-PEG polymers have been widely used for medical applications.[24,25] SDS-PAGE was performed to confirm the successful conjugation of the DSPE-PEG-NHS linker to CD34 antibodies (Figure S1). After polymer modification, the antibodies ran slowly and protein–polymer building blocks were confirmed by the absence of discrete, free protein bands in the SDS–PAGE gels, compared with native antibodies. Then, the obtained DSPE-PEG-CD34 was introduced to the platelets by the interaction between DSPE groups and the platelet membrane. To demonstrate the presence of CD34 antibodies on platelets, goat anti-mouse gold nanoparticles (10 nm) and FITC-labeled secondary antibodies were used to recognize the mouse origin CD34 antibodies on the platelets (Figure 1A–C). Fluorescence microscopy imaging results were consistent with the TEM results. FITC-labeled secondary antibodies recognized and bound to CD34 antibodies on platelets (Figure S2). DLS revealed that P-CD34 had a uniform size distribution (Figure 1D). Furthermore, ELISA showed that there were up to 7.5×10^5 CD34 antibodies per platelet (Figure 1E). The expressions of platelet surface markers CD41, GPVI, and CD42b were identical before and after CD34 decoration (Figure S3), confirming the preservation of platelet-binding motifs. Overall, linking CD34 antibodies on platelets did not cause cytotoxicity.

P-CD34 Biological Properties.

To test the ability of P-CD34 to capture endogenous $CD34^+$ stem cells, we first employed an *in vitro* cell-based assay (Figure 2A). DiO-labeled P-CD34 was co-incubated with DiI-labeled endothelial progenitor cells (EPCs), which express CD34. As shown in Figure 2B, P-CD34 (green fluorescence) efficiently bound to EPCs (red fluorescence). In contrast, the P-IgG control did not have any affinity with EPCs. CD34 antibody blockage decreases the binding of P-CD34 to EPCs. We also calculated the binding ratio between platelets and EPCs to be about 28.1 ± 7.3 platelets per EPC. Furthermore, the binding potency of P-CD34 was confirmed in the presence of whole blood (Figure 2C,D).

P-CD34 Promotion of Endogenous Stem Cell Homing to Injury and Enhancement of the Proliferation of Cardiomyocytes.

Next, we tested the concept that P-CD34 could help EPCs find sites of “injury”. Control platelets (without DSPE-PEG), P-IgG-treated EPCs, or P-CD34-treated EPCs were plated onto collagen-coated surfaces with GFP-tagged HUVECs (Figure S4A). P-EPCs had a higher binding efficiency to collagen-coated surfaces (Figure S4B,C). We performed similar testing using *ex vivo* denuded vasculatures. A segment of mice aorta was isolated and

surgically scraped to expose the subendothelial matrix (Figure S5A). Microscopic imaging showed no binding of DiI-labeled P-EPCs or EPCs on control (nondenuded) aortas (Figure S5B). Interestingly, P-EPCs had robust binding to denuded aorta, while control EPCs did not (Figure S5C). As a safety measure, aggregometry revealed that P-CD34 did not cause thrombosis even with the presence of platelet agonist collagen (Figure S6). Like many other adult stem cells, CD34-positive EPCs exert their therapeutic benefits mainly through their paracrine secretion. To test this, neonatal rat cardiomyocytes (NRCMs) were co-cultured with P-CD34 alone or conditioned medium (CM) from P-CD34 pretreated EPCs. As an indicator of proliferation, Ki67-positive cardiomyocytes were quantified. As shown in Figure S7, CM treatment increased the number of Ki67-positive NRCMs.

P-CD34 Injection Promotion of Endogenous Repair in the Infarcted Heart.

To confirm the therapeutic potential of P-CD34 in vivo, a mouse LAD ligation model was employed to create the MI. Triphenyltetrazolium chloride (TTC) staining confirmed the reproducibility of this MI model (Figure S8). After intravenous injection, a sizable portion of DiR-labeled P-CD34 accumulated in the infarct area (Figure 3), while there was still an off-targeting signal in the liver and the lungs. More importantly, compared to the injured heart, P-CD34 would not home to the normal heart. The mice were pre-injected with G-CSF intravenously for 3 days before various treatments (as described in Figure 4A) to increase the number of EPCs in the bloodstream. Furthermore, we studied the systemic inflammatory cytokine level change upon G-CSF stimulation using a cytokine array. The results showed only CCL9 and CXCL13 were elevated after G-CSF treatment (Figure S9). Therapeutic agents were given after G-CSF stimulation. P-CD34 injection had a minimal effect on the number of platelets in the whole blood (Figure S10). The capture efficiency of P-CD34 was about 33.6% (Figure S11). Next, the therapeutic efficiency was studied. The number of Ki67-positive cardiomyocytes in the peri-infarct region of P-CD34 treated hearts was higher than that of the hearts treated by the other groups (Figure 4B,C). Furthermore, the immunohistochemistry staining results of phosphorylated histone H3 (pH3), a specific marker of late G2/mitosis, and Aurora B kinase (AURKB), a marker of cytokinesis, were consistent with the Ki67 results. P-CD34 treatment increased the number of pH3- and AURKB-positive cardiomyocytes in the peri-infarct zone (Figure S12). Taking together, these results indicated that with P-CD34 treatment cardiomyocytes not only entered cell cycle but also underwent cytokinesis. In addition, the infusion of P-CD34 increased the number of von Willebrand factor (vWF)-positive vasculatures in the post-MI heart (Figure 4D,E). Masson’s trichrome staining revealed apparent heart morphology protection with the highest amount of viable myocardium in P-CD34-treated hearts compared with control-injected hearts 4 weeks after treatment (Figure 5A,B). In addition, compared with the other groups, treatment with P-CD34 led to a reduction of left ventricular end diastolic volume (LVEDV) and end systolic volume (LVESV) (Figure 5C,D). As indicators of cardiac functions, left ventricular ejection fraction (LVEF) and fractional shortening (FS) were also measured at baseline (4 h post-infarct) and 4 weeks afterward. Significant improvement in LVEFs and FSs was observed in the P-CD34 group (Figure 5E,F). These compounding results demonstrated the therapeutic benefits of P-CD34 in acute MI.

Immunohistochemistry.

P-CD34 particles were detected in the MI region (Figure 6A,B). Furthermore, endogenous CD34 cells were increased in the hearts treated with P-CD34 (Figure 6C,D), suggesting that the effective targeting of those cells to the injured heart. P-CD34 therapy did not increase the number of CD8-positive T cells and CD68-positive or F4/80-positive macrophages in the post-MI heart (Figures S13 and S14).

In the present study, we fabricated antibody-engineered platelets for the treatment of acute MI. We excised the concept of endogenous stem cell targeting, CD34-armed platelets (P-CD34) effectively captured CD34-positive circulating stem cells and guided them into the infarct area. P-CD34-linked EPCs were able to bind denuded (injured) blood vessels *ex vivo* and enhanced the targeting of endogenous stem cells to the MI injury site. Intravenous injection of P-CD34 mitigated left ventricle remodeling and promoted cardiomyocyte function in a mouse model of acute MI.

Despite considerable resources and efforts having been dedicated over the past decade to study the bioactivity of stem cells and examine their potentiality for clinical intervention, the clinical effects are not yet satisfactory. A major limitation for stem-cell-based therapy is the low efficacy of integration and retention of injected cells within the injured myocardium. It is well established that endogenous stem cells are stimulated and released from the bone marrow into the circulation. However, these released cells insufficiently homed to the injured myocardium to exert therapeutic benefits. To those ends, we conjugated CD34 antibodies with infarct-homing platelets to capture endogenous stem cells and delivered them to the MI area.

To demonstrate this strategy, we first modified CD34 antibodies using a DSPE-PEG-NHS linker. DSPE is a polymer capable of linking to the platelet membrane with high efficiency. However, the introduction of DSPE polymer–protein building blocks raises concerns over nonspecific interference and disruption of the platelet membranes, which are essential for the targeting strategy. To prove the integrity of the platelet membranes, we analyzed platelet surface markers CD41, GPVI, and CD42b, before and after modification with DSPE-PEG-CD34, using flow cytometry. The results indicated that CD34 antibody linking did not cause cytotoxicity to platelets. Platelets have an innate ability to home to injured vasculatures. Our results indicated P-CD34-pretreated EPCs exhibited superior binding to collagen surfaces in vitro and vascular lesions on denuded aortas *ex vivo*. Systemic delivery by intravenous infusion is minimally invasive but suffers from nonspecific distribution to nontarget organs. To further confirm the homing ability of platelets, we intravenously administrated P-CD34 into MI mice and verified that P-CD34 had a better homing capacity to infarcted heart compared to a normal heart. Also, a corresponding increase in signal was observed in the liver, which indicated that the particles were eventually taken up by the reticuloendothelial system (RES).[26] The off-targeting effect was consistent with previously reported studies on antibody- or peptide-based drug delivery systems. Finally, heart histology suggested that P-CD34 treatment enhanced angiomyogenesis and cardiomyocyte proliferation, resulting in the largest amount of viable myocardium and the smallest scar size among all treatment groups. Histology confirmed the recruitment of CD34-positive cells to the infarct area. One

limitation of our strategy is that CD34 is also expressed in other cells such as dendritic cells, endothelial cells, and some solid tumor cells. Thus, targeting molecules that have higher specificity to stem cells would warrant further investigation.

Taking advantage of the natural infarct-homing ability of platelets and regenerative capacity of endogenous stem cells, we engineered a new class of regenerative platelets for effective heart repair. Our design overcomes several limitations of conventional cell therapy, including unfavorable biodistribution and poor cell retention. We demonstrated that P-CD34 can effectively target endogenous stem cells to the injured heart for effective heart repair.

Supplementary Material

Refer to Web version on PubMed Central for supplementary material.

ACKNOWLEDGMENTS

K.C., Z.L., and D.S. designed the overall experiments. D.S., Z.L., S.H., K.H., T.S., H.L., and F.L. performed the experiments and analyzed the data. K.C. and Z.L. wrote the article. All authors read and approved the final article. All authors have provided the corresponding author with written permission to be named in the article. The authors thank J. Cores for proofreading the paper. The authors also thank Henan Province's Key Laboratory of Cardiac Injury and Repair for technical assistance.

Funding

This work was supported by grants from the National Institutes of Health (grant nos. HL123920 and HL137093 to K.C.), the American Heart Association (grant no. 18TPA34230092 to K.C.), the National Natural Science Foundation of China (grant no. 81873493 to D.S.), and Science and Technology Innovation Personnel of the Education Department of Henan Province (grant no. 19HASTIT002 to D.S.)

REFERENCES

(1). Feigin VL; Norrving B; Mensah GA Circ. Res 2017, 120, 439–448. [PubMed: 28154096]

(2). Khan A; Menon A; Tongers J Cell-Based Therapy in Ischemic Heart Disease In Biochemical Basis and Therapeutic Implications of Angiogenesis; Mehta JL; Mathur P; Dhalla NS, Eds.; Springer International Publishing: Cham, Switzerland, 2017; pp 343–359.

(3). Oikonomopoulos A; Kitani T; Wu JC Mol. Ther 2018, 26, 1624–1634. [PubMed: 29699941]

(4). Chen C; Termglinchan V; Karakikes I Stem Cells 2017, 35, 1131–1140. [PubMed: 28233392]

(5). Jadczyk T; Faulkner A; Madeddu P Br. J. Pharmacol 2013, 169, 247–268. [PubMed: 22712727]

(6). Tang J; Cui X; Caranasos TG; Hensley MT; Vandergriff AC; Hartanto Y; Shen D; Zhang H; Zhang J; Cheng K ACS Nano 2017, 11, 9738–9749. [PubMed: 28929735]

(7). Tang J-N; Cores J; Huang K; Cui X-L; Luo L; Zhang J-Y, Li T-S; Qian L; Cheng K Stem Cells Transl. Med 2018, 7, 354–359. [PubMed: 29468830]

(8). Schrepfer S; Deuse T; Reichenspurner H; Fischbein MP; Robbins RC; Pelletier MP Transplant. Proc 2007, 39, 573–576. [PubMed: 17362785]

(9). Barbash IM; Chouraqui P; Baron J; Feinberg MS; Etzion S ; Tessone A; Miller L; Guetta E; Zipori D; Kedes LH; Kloner RA; Leor J Circulation 2003, 108, 863–868. [PubMed: 12900340]

(10). Segers VFM; Lee RT Nature 2008, 451, 937–942. [PubMed: 18288183]

(11). Hu S; Ogle BM; Cheng K Curr. Opin. Cell Biol 2018, 54, 37–42. [PubMed: 29704858]

(12). Tang J; Wang J; Huang K; Ye Y; Su T; Qiao L; Hensley MT; Caranasos TG; Zhang J; Gu Z; Cheng K Sci. Adv 2018, 4, No. eaat9365.

(13). Su T; Huang K; Daniele MA; Hensley MT; Young AT; Tang J; Allen TA; Vandergriff AC; Erb PD; Ligler FS; Cheng K ACS Appl. Mater. Interfaces 2018, 10, 33088–33096. [PubMed: 30188113]

(14). Cui X; Tang J; Hartanto Y; Zhang J; Bi J; Dai S; Qiao SZ, Cheng K; Zhang H ACS Appl. Mater. Interfaces 2018, 10, 37783–37796. [PubMed: 30360109]

(15). Bianconi V; Sahebkar A; Kovanen P; Bagaglia F; Ricciuti A; Calabro P; Patti G; Pirro M Pharmacol. Ther 2018, 181, 156–168. [PubMed: 28827151]

(16). Cheng K; Shen D; Hensley MT; Middleton R; Sun B; Liu W; De Couto G; Marban E Nat. Commun 2014, 5, 4880. [PubMed: 25205020]

(17). Dehaini D; Wei X; Fang RH; Masson S; Angsantikul P; Luk BT; Zhang Y; Ying M; Jiang YJ; Kroll AV; Gao W; Zhang L Adv. Mater 2017, 29, 1606209.

(18). Zhang X; Wang J; Chen Z; Hu Q; Wang C; Yan J; Dotti G; Huang P; Gu Z Nano Lett 2018, 18, 5716–5725. [PubMed: 30063143]

(19). Tang J; Su T; Huang K; Dinh P-U; Wang Z; Vandergriff A; Hensley MT; Cores J; Allen T; Li T; Sproul E; Mihalko E; Lobo LJ; Ruterbories L; Lynch A; Brown A; Caranasos TG; Shen D; Stouffer GA; Gu Z; Zhang J; Cheng K Nat. Biomed. Eng 2018, 2, 17–26. [PubMed: 29862136]

(20). Su T; Huang K; Ma H; Liang H; Dinh P-U; Chen J; Shen D; Allen TA; Qiao L; Li Z; Hu S; Cores J; Frame BN; Young AT; Yin Q; Liu J; Qian L; Caranasos TG; Brudno Y; Ligler FS; Cheng K Adv. Funct. Mater 2019, 29, 1803567.

(21). Li Z; Hu S; Cheng KJ Mater. Chem. B 2018, 6, 7354–7365.

(22). Wang C; Sun W; Ye Y; Hu Q; Bomba HN; Gu Z Nat. Biomed. Eng 2017, 1, 0011.

(23). Stellos K; Bigalke B; Borst O; Pfaff F; Elskamp A; Sachsenmaier S; Zachmann R; Stamatelopoulos K; Schonberger T; Geisler T; Langer H; Gawaz M Eur. Heart J 2013, 34, 2548–2556. [PubMed: 23594593]

(24). Chan JM; Zhang L; Yuet KP; Liao G; Rhee J-W; Langer R; Farokhzad OC Biomaterials 2009, 30, 1627–1634. [PubMed: 19111339]

(25). Wei T; Liu J; Ma H; Cheng Q; Huang Y; Zhao J; Huo S; Xue X; Liang Z; Liang X-J Nano Lett. 2013, 13, 2528–2534. [PubMed: 23634882]

(26). Hu C-MJ; Fang RH; Wang K-C; Luk BT; Thamphiwatana S; Dehaini D; Nguyen P; Angsantikul P; Wen CH; Kroll AV; Carpenter C; Ramesh M; Qu V; Patel SH; Zhu J; Shi W; Hofman FM; Chen TC; Gao W; Zhang K; Chien S; Zhang L Nature 2015, 526, 118. [PubMed: 26374997]

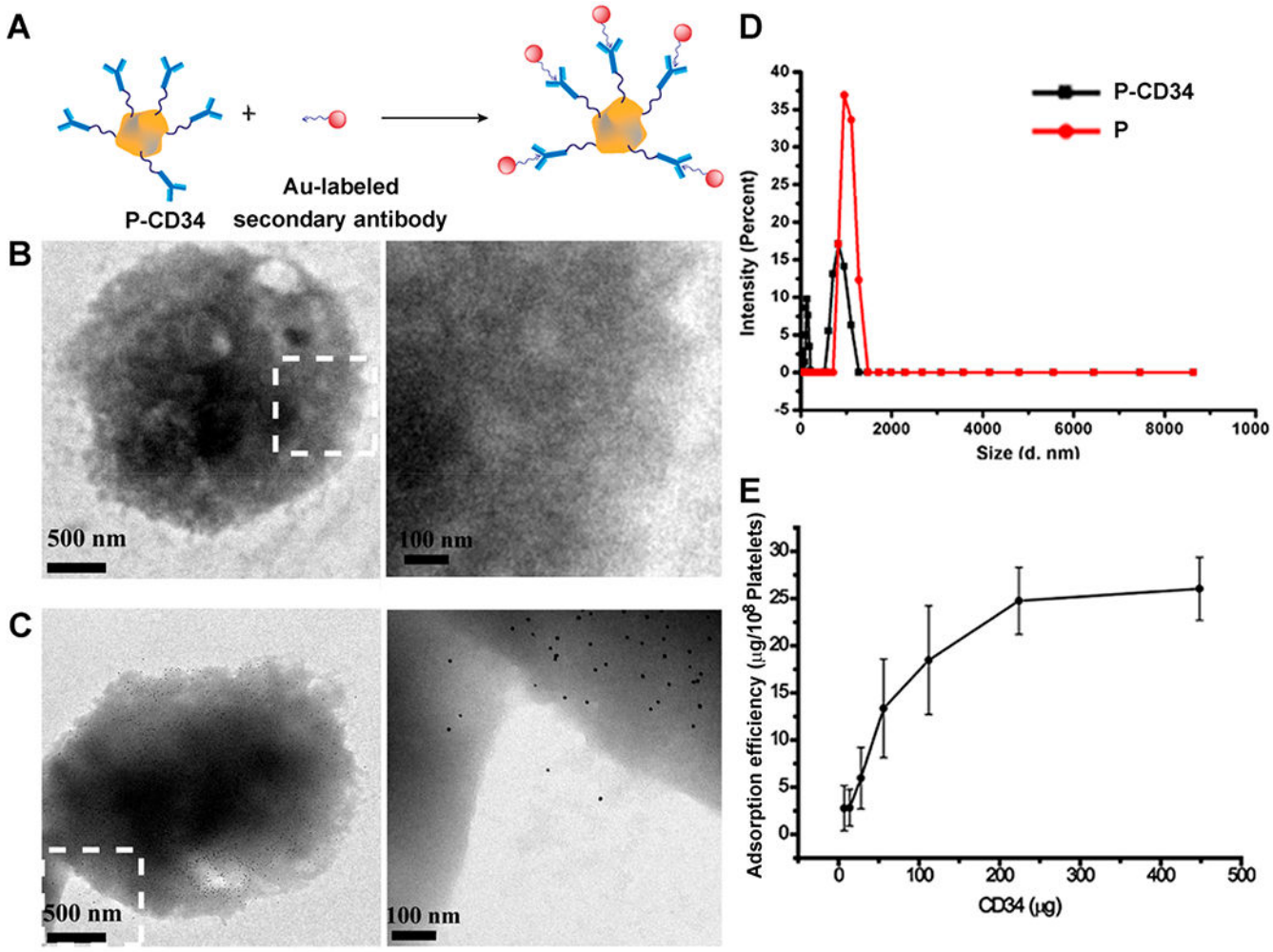

Figure 1.

Conjugation of platelets and DSPE-PEG-CD34. (A) A schematic showing the capturing of CD34-modified platelets by gold-labeled goat anti-mouse secondary antibodies. (B, C) TEM images of platelets and P-CD34 incubated with gold-labeled secondary antibodies. (D) DLS analysis of platelets before and after DSPE-PEG-CD34 conjunction. (E) Determination of the amount of CD34 antibodies on platelets.

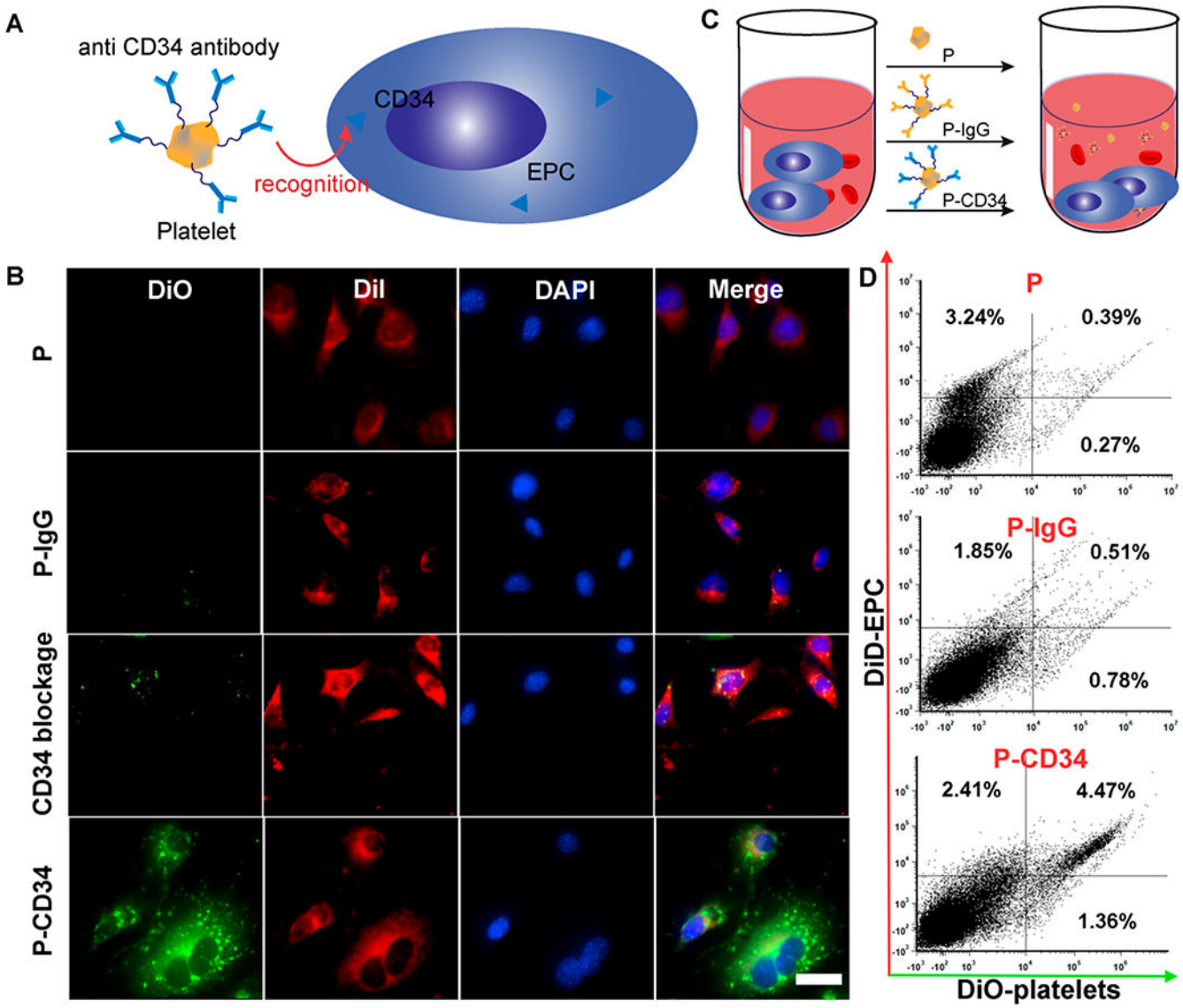

Figure 2.

Binding efficiency of P-CD34 to EPCs. (A) A schematic showing the experimental design for P-CD34 targeting to EPCs. (B) Fluorescent micrographs confirming the ability of P-CD34 to capture EPC. DiI-labeled EPC were incubated with platelet, P-IgG, and P-CD34. CD34 blockage was used as a control. (C) Schematic showing the experimental design for capturing EPCs in whole blood using different samples. (D) Flow cytometry analysis showing the ability of P-CD34 to capture EPCs in whole blood. The 10^5 DiI-labeled EPCs were mixed with the whole blood before the addition of different capturing agents. Scale bar: 10 μm

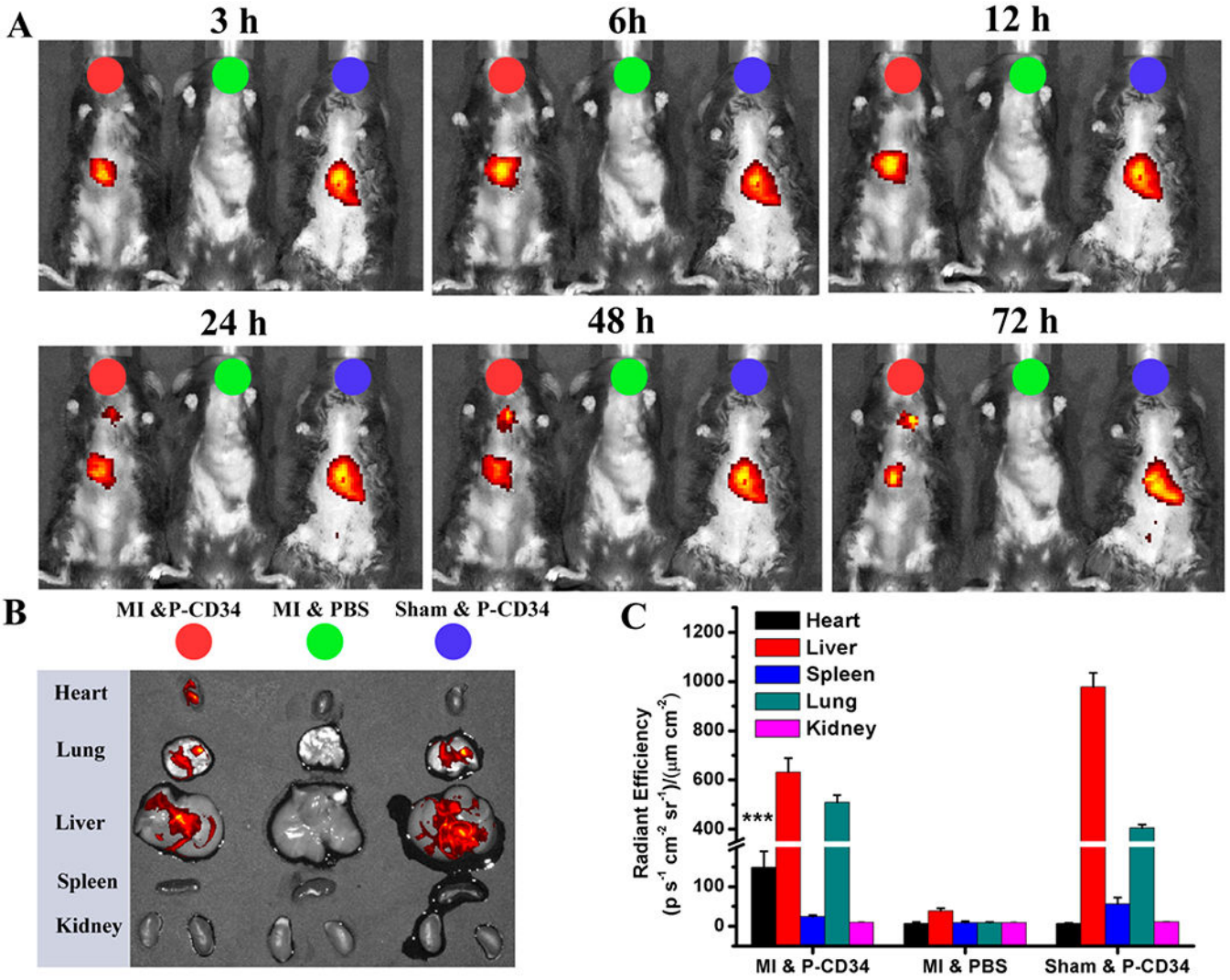

Figure 3.

Biodistribution of P-CD34 in mice with acute MI. (A) In vivo fluorescent imaging of MI mice or sham mouse at various time interval after intravenous injection of DiR-labeled P-CD34 or PBS. (B) Ex vivo fluorescent imaging of the major organs from the treated animals. (C) Quantitative analysis of fluorescent intensity in the organs. P-CD34 treated groups vs other groups. Triple asterisks indicate $P < 0.005$.

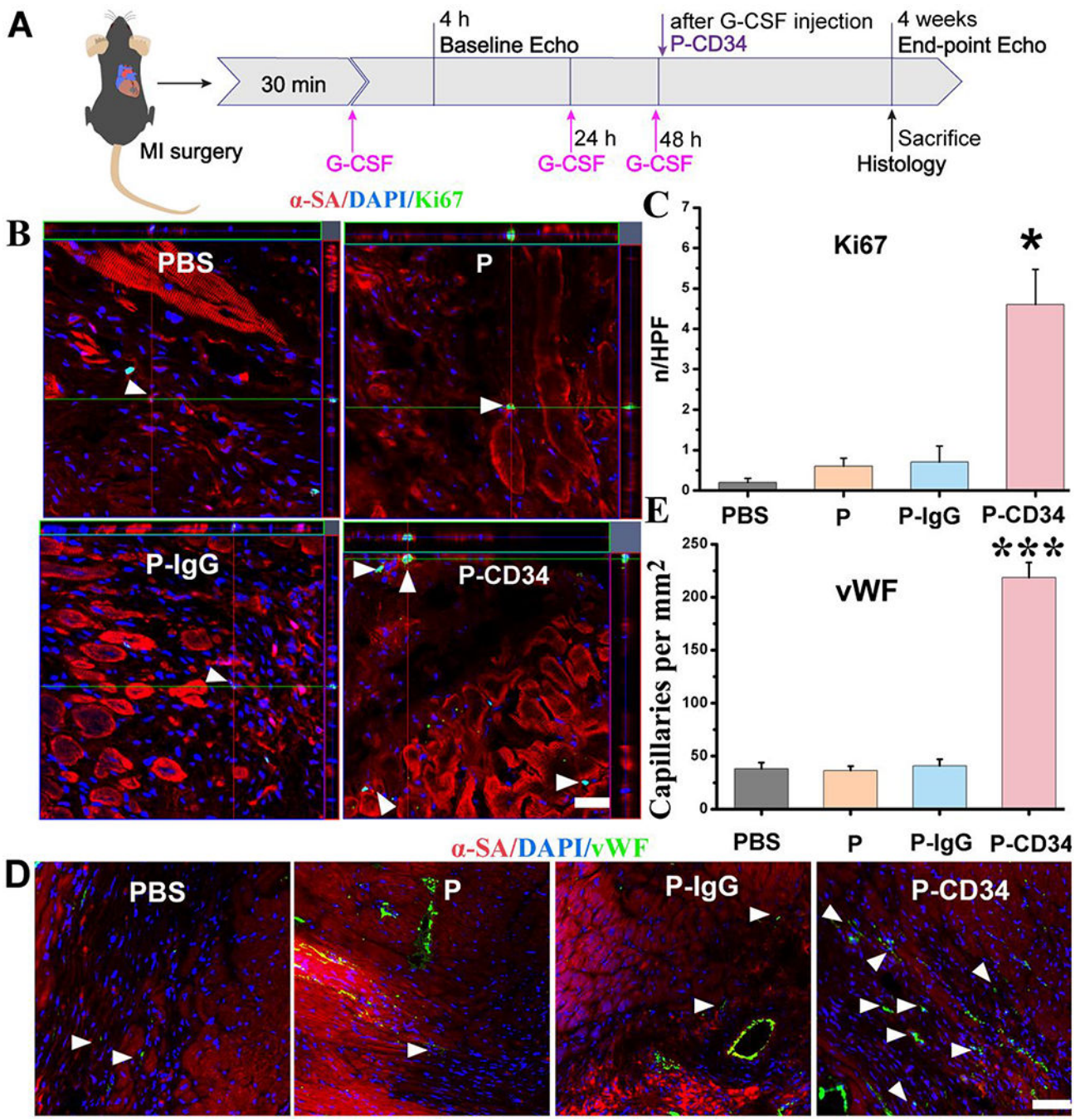

Figure 4.

P-CD34 promotion of cardiac repair in a mouse model of heart attack. (A) A schematic showing the animal study design. (B) Z-stack analysis showing Ki67+ nuclei are embedded within cardiomyocytes treated by PBS, platelets, IgG-modified platelets, or CD34-attached platelets 4 weeks later. White arrowheads indicate the positively stained cells. (C) Quantitative analysis of Ki67-positive nuclei. (D) Representative micrographs showing vWF-labeled blood vessels (green) in sample groups (control PBS and hearts treated with platelets, IgG-modified platelets, or CD34-attached platelets) 4 weeks later. White

arrowheads indicate the positively stained cells. White arrowheads indicate vWF-positive capillary density in the infarcted area. (E) Quantitative analysis of vWF-positive vasculatures. Scale bar: 20 μm, P-CD34 groups vs other groups. Single asterisks indicate $P < 0.05$, and triple asterisks indicate $P < 0.005$.

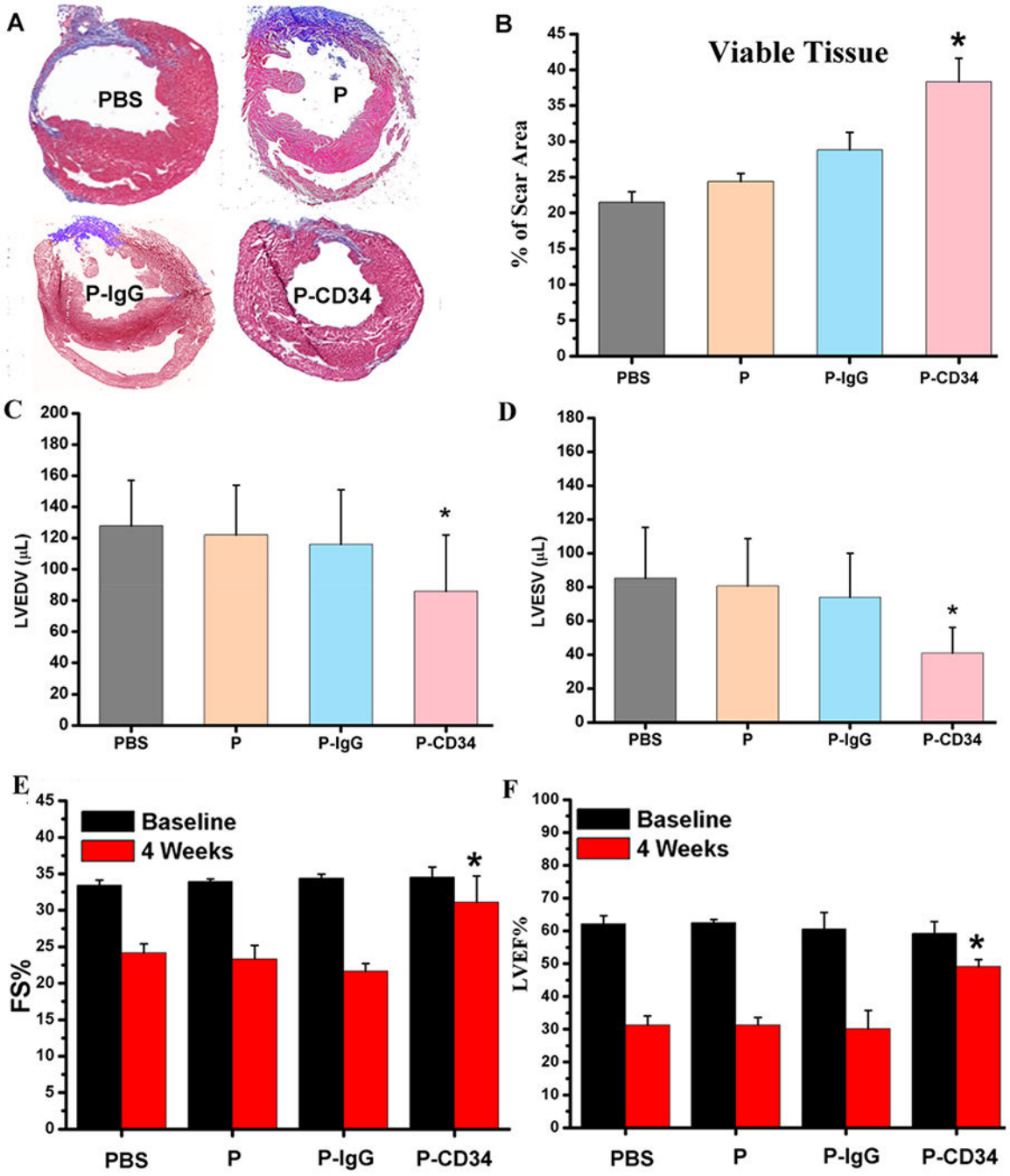

Figure 5.

Functional benefits of P-CD34 therapy. (A) Representative Masson's trichrome-stained myocardial sections 4 weeks after treatment. (B) Quantitative analyses of viable myocardium from the Masson's trichrome images (n = 6 animals per group). (C, D) Left ventricular end diastolic (C) and end systolic (D) volumes (LVEDV and LVESV) measured by echocardiography at 4 weeks (n = 6 animals per group). (E, F) Left ventricular fractional shortening (LVFS) and ejection fractions (LVEFs) were measured by echocardiography at baseline and 4 weeks later. (n = 6 animals per group). All data are presented as mean plus or

minus the standard deviation. Single asterisks indicated P-CD34 groups vs other groups and $P < 0.05$.

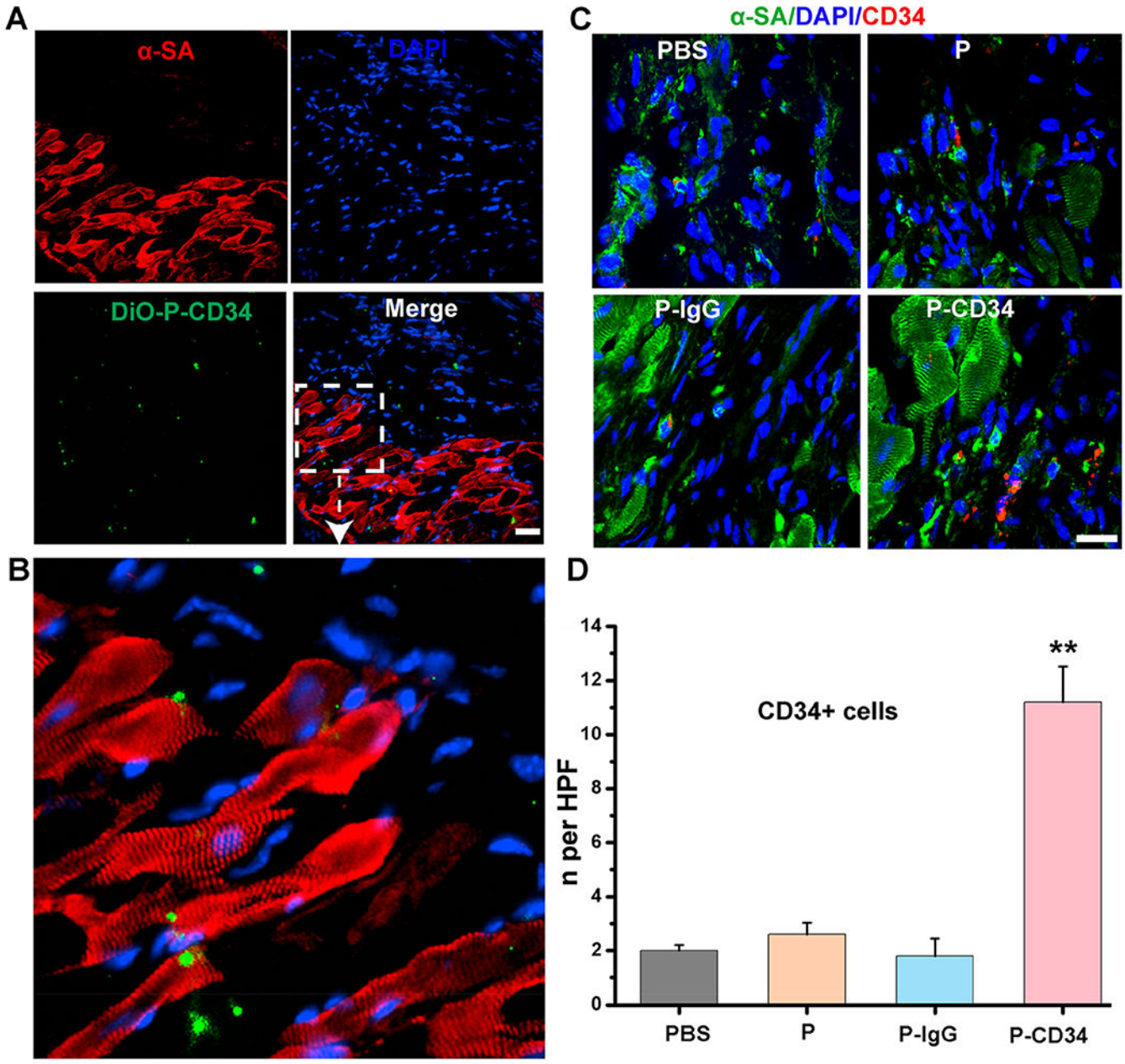

Figure 6.

Evaluation of the mechanism for improved treatment effects. (A) Fluorescent micrographs confirming the ability of P-CD34 to target the MI area. (B) The enlarged image of panel A. (C) Representative images showing CD34-positive cells in hearts treated with control PBS, platelets, IgG-modified-platelets, or CD34-attached-platelets at 4 weeks. (D) Quantitative analysis of the number of CD34-positive cells. Scale bar: 20 μm; P-CD34 groups vs other groups; double asterisks indicate $p < 0.01$.

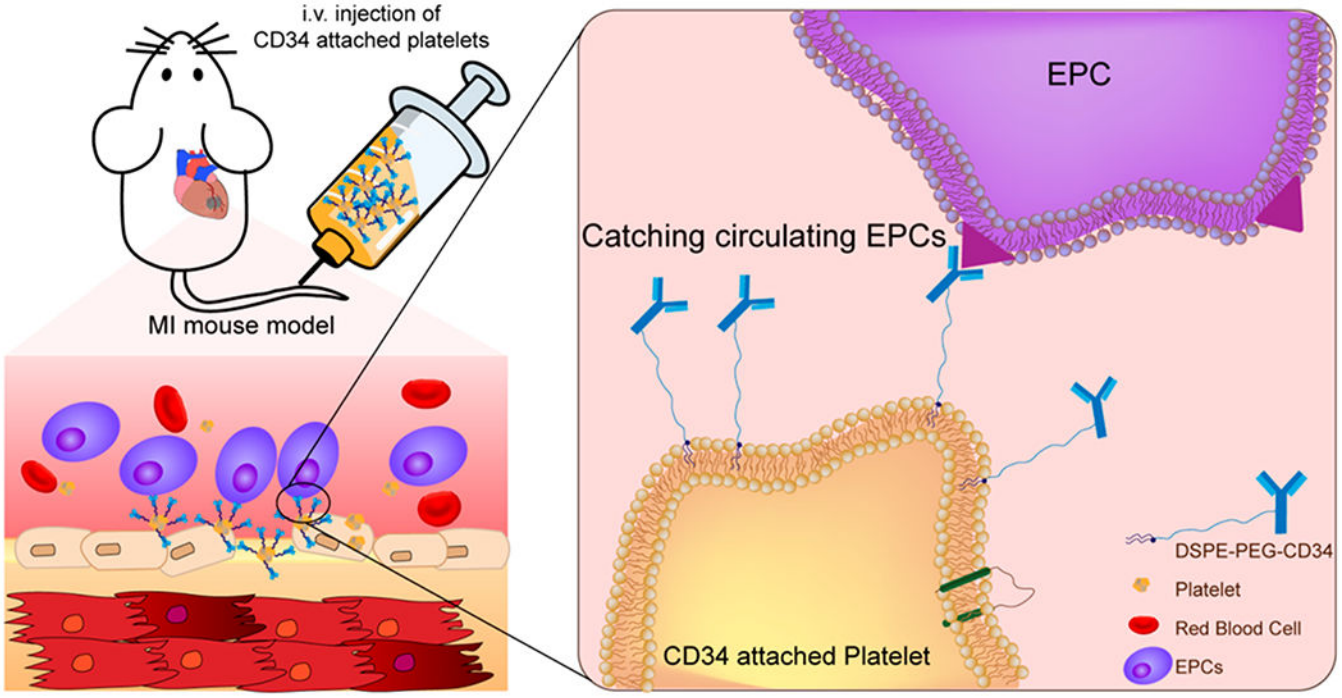

Scheme 1.

Schematic Showing the Concept of Engineered Platelets for Targeting Endogenous Stem Cells